Discover Oncology

Research

Combination treatment with Phloretin enhances the anti-tumor efficacy of radiotherapy in lung cancer models

Juan Tang[1] · Weijie Xiong[2] · Xianguo Liu[1] · Yuhui Shi[1] · Yanxin Yu[1] · Maolin Shi[1] · Hongyu Xu[1]

Received: 15 January 2025 / Accepted: 25 April 2025
Published online: 07 May 2025

Abstract

Introduction Phloretin (Ph), an apple polyphenol, has been shown to possess anti-tumor effects. This study aimed to investigate the anti-tumor effects of the combination of Ph and radiotherapy on lung cancer.

Methods The proliferative rate of Lewis lung carcinoma (LLC) cells treated with Ph was evaluated using the MTT assay. The radiosensitization effect of Ph was assessed using the clone formation assay. Additionally, the anti-tumor and radiosensitization effects of Ph were explored in LLC xenografts in mice.

Results Ph inhibited the proliferation of LLC cells in a time- and dose-dependent manner ($p < 0.05$). Moreover, the combination of Ph with radiotherapy significantly inhibited LLC cell colony formation ($p < 0.05$). In vivo studies demonstrated that the combination of Ph with radiotherapy significantly inhibited tumor growth, achieving a tumor inhibition rate of 74.44% compared to the control group ($p < 0.01$). This combination also prolonged the median survival times of mice by 31 days compared to the control group ($p < 0.01$), reduced tumor glucose uptake, promoted tumor cell apoptosis, and suppressed tumor cell proliferation.

Conclusion This study suggests that the combination of Ph with radiotherapy exhibits promising activity against lung cancer, potentially through mechanisms including inhibition of glucose transport and promotion of apoptosis. These findings may provide a new therapeutic strategy for improving lung cancer treatment.

Keywords Phloretin · Radiotherapy · Radiosensitization · Lung cancer

1 Introduction

Lung cancer is the main cause of cancer-related mortality worldwide, with an estimated 1.8 million deaths (18%), followed by colorectal cancer (9.4%) and liver cancer (8.3%) [1, 2]. GLOBOCAN estimated that there were 2,480,301 new lung cancer cases (12.4% of all cancers) and 1,817,172 death cases (18.7% of all cancers) in 2022, with the highest incidence and mortality rate in the world [3]. Smoking is the most important risk factor, and about 10% of smokers will eventually develop lung cancer [1]. Despite significant advances in lung cancer biology, screening techniques, and treatment, the prognosis of lung cancer remains poor, with an overall 5-year survival rate varying from 4 to 17% depending on stage

Juan Tang and Weijie Xiong have contributed equally to this work.

✉ Hongyu Xu, Hongyu_xudoctor@163.com; Juan Tang, 15181966133@163.com; Weijie Xiong, xiongweijie427@163.com; Xianguo Liu, doclxg@163.com; Yuhui Shi, 184703248@qq.com; Yanxin Yu, yuyanxin0417@163.com; Maolin Shi, elcymoly@yeah.net | [1]Department of Oncology, 363 Hospital, No. 108 Daosangshu Street, Wuhou District, Chengdu 610041, Sichuan, China. [2]Department of Oncology, Chengdu Fifth People's Hospital, Affiliated Fifth People's Hospital of Chengdu University of Traditional Chinese Medicine, Cancer Prevention and Treatment Institute of Chengdu, Chengdu, China.

and regional differences [4, 5]. Radiotherapy is the principal therapy for lung cancer; however, radiotherapy resistance often limits its efficacy [6]. Therefore, the combination of drugs with radiotherapy to enhance the therapeutic effect of radiotherapy is gaining more attention.

Phloretin (Ph), whose chemical structure is 3-(4′-hydroxyphenyl)-1-(2,4,6-trihydroxyphenyl) propan-1-one, belongs to the dihydrochalcones family of flavonoids and is present in the peel of the apple (80–420 mg/kg) and pulp (16–20 mg/kg) [7]. Ph has been shown to exhibit anti-tumor effects on various types of tumors [8, 9]. Kapoor et al. reported that Ph inhibited proliferation and induced apoptosis in colorectal carcinoma cells by halting the cell cycle at G2/M stages and regulating the expression of Bax and Bcl-2 [10]. Ph combined with atorvastatin exerts a strong synergistic effect in suppressing colon cancer cell growth via TRAIL-induced apoptosis and cell cycle arrest at the G2/M checkpoint [11, 12]. In breast cancer cells, Ph exhibited the anti-proliferation effect through inhibition of type 2 glucose transporter (GLUT2) [13]. Although previous studies have demonstrated Ph's anti-tumor effects in colon and breast cancers through GLUT-mediated metabolic modulation, its role in lung cancer remains unexplored. To our knowledge, no prior research has investigated the combined effects of Ph with radiotherapy in lung cancer models. However, several studies have shown that other flavonoids can enhance the radiosensitivity of cancer cells. For example, rhamnetin, a derivative of quercetin, has been suggested to influence the Notch-1 signaling pathway in NCI-H460 and NCI-H1299 cells, thereby improving their radiosensitivity [14]. Rhamnetin has been shown to inhibit epithelial-mesenchymal transition (EMT) and decrease Notch-1 expression, which subsequently induced apoptosis by dampening the NF-κB pathway [14, 15]. Similarly, isorhamnetin, another metabolite of quercetin, has also been reported to enhance the radiosensitivity of lung cancer cells [16]. These findings underscore the potential of combining flavonoids with radiotherapy to improve treatment outcomes.

Based on the above context, we hypothesized that Ph might participate in the alleviation of lung cancer and enhance the radiosensitivity of lung cancer in vivo. In this study, the anti-tumor effects of Ph combined with radiotherapy were evaluated using Lewis lung carcinoma (LLC) xenografts in mice. Our study may provide a potential new treatment approach for lung cancer, especially through the combination of flavonoid functional ingredients and radiotherapy.

2 Materials and methods

2.1 Cell culture and animals

The LLC cells were provided by the Cancer Center and State Key Laboratory of Biotherapy, West China Hospital of Sichuan Province, and cultured in Dulbecco's Modified Eagle Medium (DMEM, MeiLun Co. Ltd., Dalian, China) supplemented with 10% fetal bovine serum (FBS, MeiLun Co. Ltd., Dalian, China) at 37 °C in a 5% CO_2 incubator.

Forty-eight female C57BL/6 J mice, 5 weeks old, were purchased from Chengdu Dashuo Biotechnology Co. Ltd. and maintained under specific pathogen-free (SPF) conditions. All animal experiments were carried out following the guidelines of the Institutional Animal Care and Use Committee of the West China Hospital of Sichuan.

2.2 Cell toxicity assay

The MTT assay (Sigma-Aldrich Inc., Missouri, USA) was utilized to examine the anti-proliferative effect of Ph on the LLC cells. The vehicle of Ph used in LLC cells was normal saline. 200 µl cell suspension (1×10^7cells/ml) was seeded into the 96-well plate and treated with different concentrations of Ph (50, 100, 150, 200 µg/ml) at 37 °C with 5% CO_2 for 12, 24, and 36 h. Then, 200 µl MTT solution (5 mg/ml) was added to the treated cells and incubated for 4 h. Subsequently, 200 µl of dimethyl sulfoxide (DMSO, Sigma-Aldrich Inc., Missouri, USA) was added to dissolve the purple formazan. Absorbance at 480 nm was measured using the microplate reader, and the cell survival rate was calculated based on the absorbance values. Each experimental group was repeated six times.

2.3 Colony forming assay

The colony forming assay was performed to evaluate the sensitivity of LLC cells to Ph or radiotherapy. Ph (50 µg/ml) was added to LLC cells for 1 h, and the cells were irradiated with 2, 4, 6, 8, and 10 Gy using a linear accelerator (Varian, California, USA) at the dose rate of 60 cGy/min for 1 h. Then, the treated cells were seeded into six-well plates and cultured in fresh drugs-free medium for 10–14 days. Next, the cells were washed twice with PBS, fixed with methanol, and stained with 0.5% crystal violet for 20 min (Sigma-Aldrich Inc., Missouri, USA). The number of colonies was counted using a

Leica TE2000-S microscope (Leica Microsystems, Wetzlar, Germany). Plating efficiency (PE), surviving fraction (SF), and sensitivity enhancement ratio (SER) were calculated using nonlinear regression to fit the data with a multi-target model.

2.4 Establishment of lung cancer mice model and treatments

To establish the lung cancer model, 100 µl of cell suspension (2×10^7 cells/ml) was injected into the right outer thigh of mice. The thigh region's abundant blood supply and tumorigenic potential favored tumor formation and growth. Additionally, a cell concentration of 2×10^7 cells/ml has consistently resulted in good tumor models in previous experiments [17]. When the tumors reached approximately 100–200 mm^3, mice were randomly divided into 4 groups (n = 12 per group): (i) control group (0.9% normal saline), (ii) Ph treatment alone group, (iii) radiotherapy alone group, and (iv) Ph combined with radiotherapy group. Based on the studies of Hsiao et al. and Min et al., 0.9% normal saline and Ph (20 mg/kg) solutions were injected intraperitoneally every two days for 12 days [18, 19]. Before the third injection, the tumor-bearing mice were irradiated with a total dose of 10 Gy at a rate of 60 cGy/min, with a source-to-subject distance of 70 cm. Tumor volume was measured using vernier calipers for up to 20 days. After 20 days of treatment, half of the mice in each group were anesthetized with 1% pentobarbital at a dose of 5 ml/kg and subsequently euthanized via cervical dislocation. Following this, tumor sizes were measured. The remaining six mice in each group were used to record survival time.

2.5 *Micro ^{18}F-FDG positron emission tomography/computed tomography (PET/CT) imaging*

After treatment, the metabolic status in tumors was evaluated by measuring ^{18}F-FDG uptake through the Inveon micro-PET/CT (Siemens, Munich, Germany). After fasting for 12 h, mice were anesthetized with 1% pentobarbital at a dose of 5 ml/kg and then injected with 100–200 mCi FDG in the tail vein. The regions of interest (ROI) were drawn on the right foot. Then, the standard uptake value (SUV) was calculated in the ROI to quantify tumor uptake of glucose.

2.6 Apoptosis assay

The cell apoptosis was assessed using the Annexin V-FIFC Apoptosis Detection kit (BD Biosciences, New Jersey, USA). The soya-sized tumors were digested into single-cell suspensions and immediately resuspended in 200 µl of 0.25% trypsin/EDTA (1:1, v/v) at room temperature for 1 min. Cell clusters and debris were filtered using the 70 mm nylon mesh filter. Then, the supernatant was removed by centrifuging at 1,500 rpm for 3 min at room temperature, and cells were washed three times with saline. The cells were resuspended in 500 µl binding buffer (1×10^6 cells/ml). 5 µl propidium iodide and 5 µl Annexin V-FITC were added and incubated in the dark at room temperature for 15 min. Finally, the apoptotic cells were detected by the flow cytometry (BD Biosciences, New Jersey, USA).

2.7 Immunohistochemistry (IHC)

The tumor tissues were fixed in 10% neutral buffered formalin at 4 °C for 6 h and embedded in paraffin. The tumor tissues were sectioned into 4-µm-thick sections and stained with anti-Ki-67 antibody (Bioworld Technology Co. Ltd., Nanjing, China, 1:100) according to the manufacturer's instructions. The samples were observed under a 400 × magnification on Leica TE2000-S microscope (Leica Microsystems, Wetzlar, Germany). Ki-67-positive cells and total cell numbers were counted in five randomly selected fields of view, and the percentage of positive cells was calculated.

2.8 Statistical analysis

Statistical analysis was performed using SPSS Statistics version 17.0 software (SPSS Inc., Illinois, USA). All data are presented as the mean ± standard deviation (SD). Normality was assessed using the D'Agostino-Pearson test, and homogeneity of variance was evaluated using Bartlett's test. For comparing different groups, one-way analysis of variance (ANOVA) was conducted, followed by post-hoc tests. Specifically, Tukey's HSD test was used for pairwise comparisons when the data met the assumptions of normality and homogeneity of variances. For survival analysis, Kaplan–Meier curves were generated, and differences in survival distributions were compared using the log-rank test. Additionally, Cox proportional hazards regression analysis was performed to estimate the hazard ratios (HR) and 95% confidence

intervals (CI) for each treatment group compared to the control group. A *p*-value less than 0.05 was considered statistically significant.

3 Results

3.1 Ph significantly inhibited LLC cell proliferation

The anti-proliferative efficacy of Ph on LLC cells was evaluated. As shown in Fig. 1A, the LLC cell viability decreased with increasing concentrations of Ph. Furthermore, at the same concentration of Ph, the lowest cell viability was observed in those treated for 36 h (Fig. 1B). These results indicated that Ph significantly inhibited the proliferation of LLC cells in a dose- and time-dependent manner. Additionally, Ph concentrations below 50 μg/ml did not significantly inhibit the proliferation of LLC cells. Therefore, we selected a concentration of 50 μg/ml for Ph based on the dose–response curves, as it showed moderate anti-proliferative effects on LLC cells. This concentration was chosen for subsequent analyses to further investigate its biological effects.

3.2 Ph combined with radiotherapy inhibited colony formation of LLC cells

The radiosensitization effect of Ph at different irradiations (2, 4, 6, 8, and 10 Gy) was evaluated through Colony forming assay. The results revealed that colony formation rates of LLC cells gradually decreased as the irradiation dose increased (Fig. 2). At the same irradiation dose, the colony formation rates of LLC cells in the combination of Ph and radiotherapy group were significantly decreased compared to the radiotherapy group (Fig. 2A). The survival curves of LLC cells were calculated by a multi-target model, and we found that the survival curve in the combination of Ph and radiotherapy group was down-shifted compared to the radiotherapy group (Fig. 2B).

3.3 Ph combined with radiotherapy delayed the tumor growth and improved survival

To assess the therapeutic efficacy of Ph combined with radiotherapy in vivo, subcutaneous xenograft LLC tumors were established in C57BL/6 mice. The mice were randomly assigned to four groups of 12 mice each. Compared with the control group, tumor volumes were significantly reduced in the groups treated with Ph, radiotherapy, and the combination of Ph and radiotherapy (Fig. 3A). Specifically, the tumor inhibition rates compared to the control group were 38.99% for the Ph group ($p < 0.05$), 59.33% for the radiotherapy group ($p < 0.01$), and 74.44% for the combination group ($p < 0.01$).

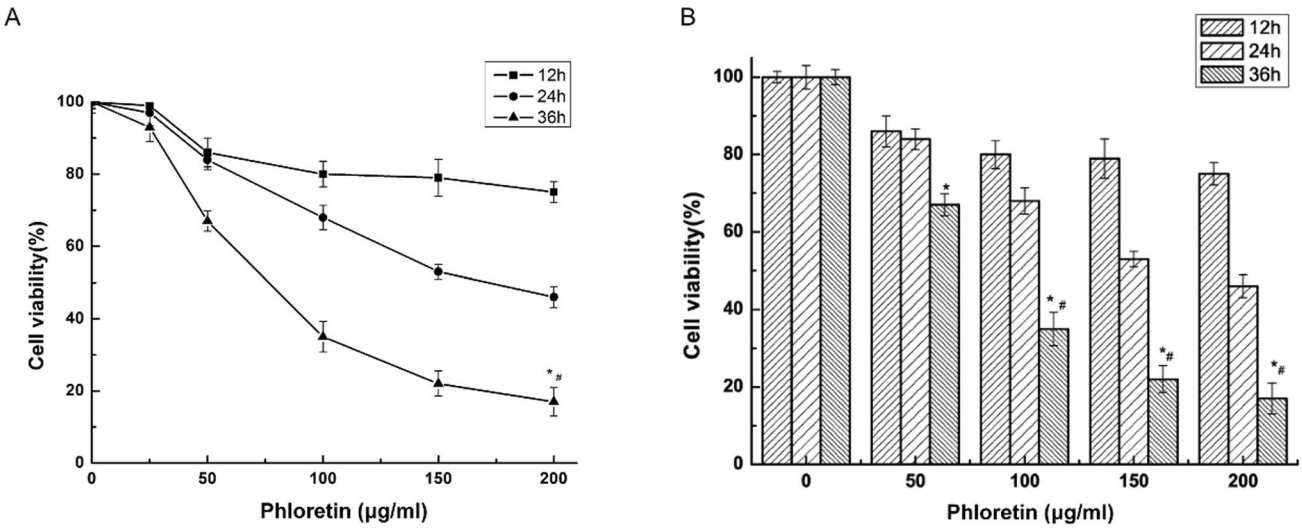

Fig. 1 Cell viability of LLC cells treated with different concentrations of Ph. **A** Phloretin inhibits the proliferation of LLC. The square represents 12 h, the circle represents 24 h, and the triangle represents 36 h. **B** Cell viability of LLC treated with different concentrations of Ph for 12, 24, and 36 h. Data are expressed as mean ± SD. *$p < 0.01$, comparing 12 h to 36 h; #$p < 0.01$, comparing 24 h to 36 h

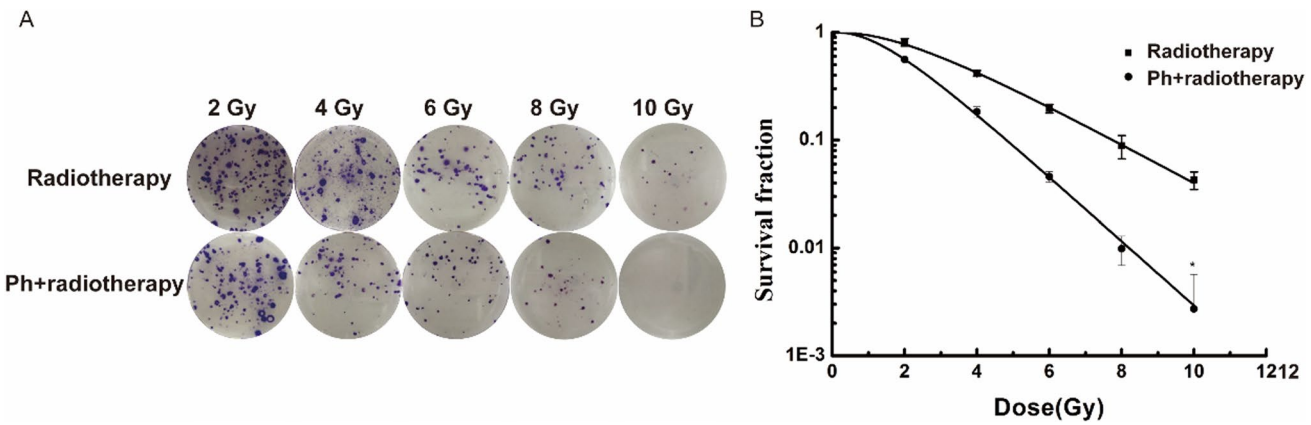

Fig. 2 Ph enhanced the radiation sensitivity of LLC cells. **A** Colony formation assay of LLC cells. **B** Survival fraction curves were generated. The square represents the radiotherapy group, and the circle represents the combination of Ph and radiotherapy group. *$p < 0.05$

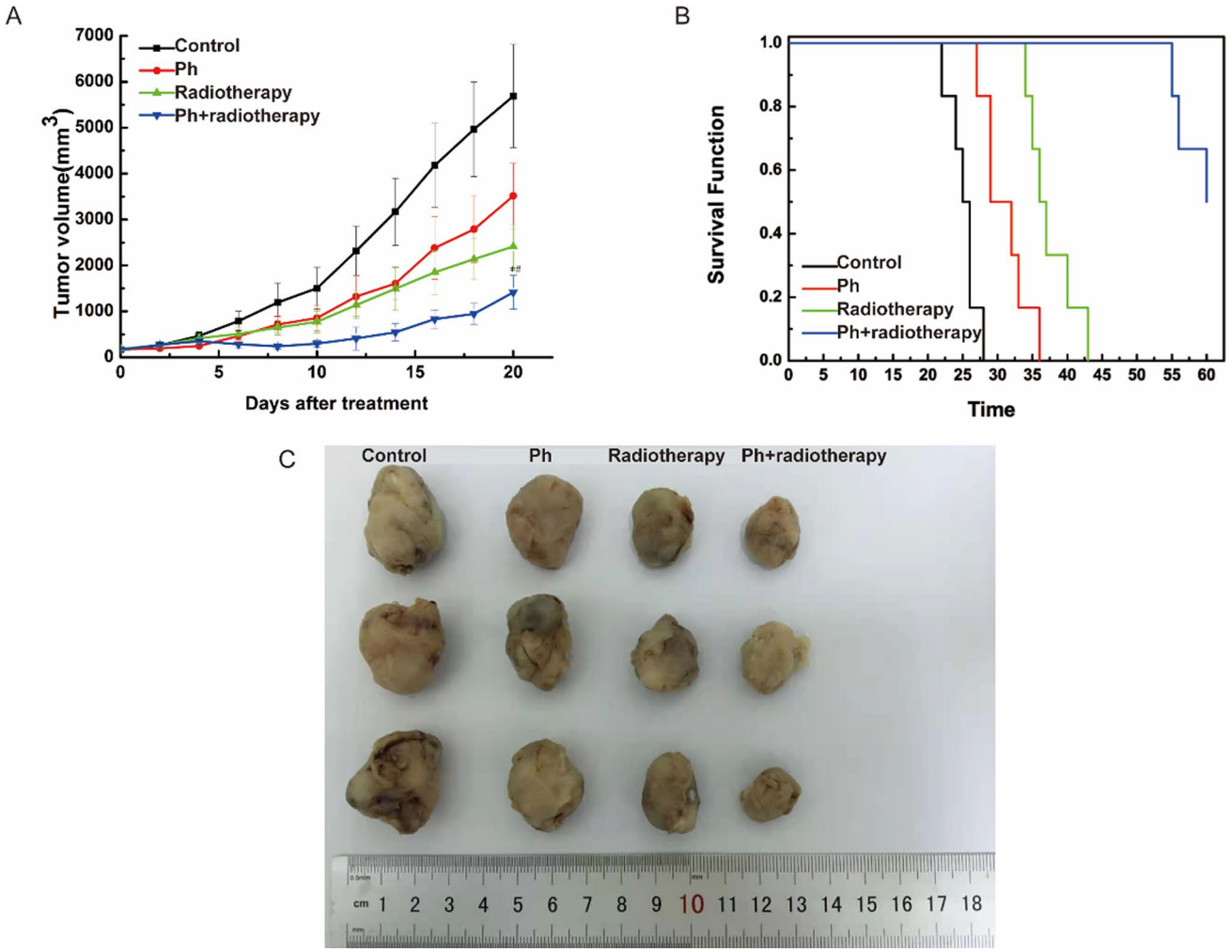

Fig. 3 Ph combined with radiotherapy inhibited LLC tumor growth in vivo. **A** Tumor growth curve of LLC xenograft mice in four groups. **B** Survival curve of LLC xenograft mice in four groups. The median survival times were 25 days for the control group, 29 days for the Ph group, 36 days for the radiotherapy group, and 56 days for the combination of Ph and radiotherapy group. **C** Tumor sizes in four groups after treatment completion. *$p < 0.01$, the combination of Ph and radiotherapy group compared to the control group; #$p < 0.01$, the combination of Ph and radiotherapy group compared to the radiotherapy group

Notably, the combination of Ph and radiotherapy group exhibited the most pronounced therapeutic effect, significantly inhibiting tumor growth (Fig. 3A). Consistently, the combination group had the smallest tumor volume among the four groups after treatment completion (Fig. 3C).

In addition to tumor volume reduction, a survival benefit was observed in the groups treated with Ph, radiotherapy, and the combination of Ph and radiotherapy. Compared with the control group, the median survival times were extended by 4 days in the Ph group, 11 days in the radiotherapy group, and 31 days in the combination of Ph and radiotherapy group (Fig. 3B). The survival benefit was further supported by the HR obtained from Cox proportional hazards regression analysis. The Ph group exhibited an HR of 0.052 (95% CI 0.006–0.468, $p = 0.008$), and the radiotherapy group showed an HR of 0.011 (95% CI 0.001–0.129, $p < 0.001$). Notably, the combination group achieved the most significant survival benefit, with an HR of 0.001 (95% CI 0.000–0.023, $p < 0.001$).

These findings suggested that combining Ph with radiotherapy significantly inhibited tumor growth and prolonged survival in the tumor-bearing mice.

3.4 *Ph combined with radiotherapy reduced ^{18}F-FDG uptake*

The ^{18}F-FDG PET/CT imaging results from four groups of tumor-bearing mice are shown in Fig. 4A. Compared to the control group, the SUVmax value of the Ph, radiotherapy, and the combination of Ph and radiotherapy groups was significantly down-regulated (Fig. 4B). Additionally, the combination of Ph and radiotherapy group exhibited the lowest mean SUVmax value of 2.05 ± 0.21, which was significantly lower than the 5.51 ± 0.26 in the Ph group and the 3.15 ± 0.17 in the radiotherapy group. These results indicated that the combination of Ph and radiotherapy had a stronger inhibitory effect on lung cancer tumor metabolism than either treatment alone.

3.5 Ph combined with radiotherapy increased apoptosis

The mechanism that Ph enhances radiosensitization in lung cancer was explored through flow cytometry. Representative flow cytometry images of apoptotic cells in four groups are shown in Fig. 5A. The highest rate of apoptotic cells was observed in the combination of Ph and radiotherapy group (39.36 ± 1.52%), followed by radiotherapy alone (23.78 ± 1.08%), Ph alone (14.63 ± 0.24%), and control groups (6.94 ± 1.68%) (Fig. 5B). The apoptosis rate of tumor cells in the combination of Ph and radiotherapy group was significantly higher than that of either monotherapy (Fig. 5B). The results suggested that Ph could promote irradiation-induced cell apoptosis in tumor-bearing mice.

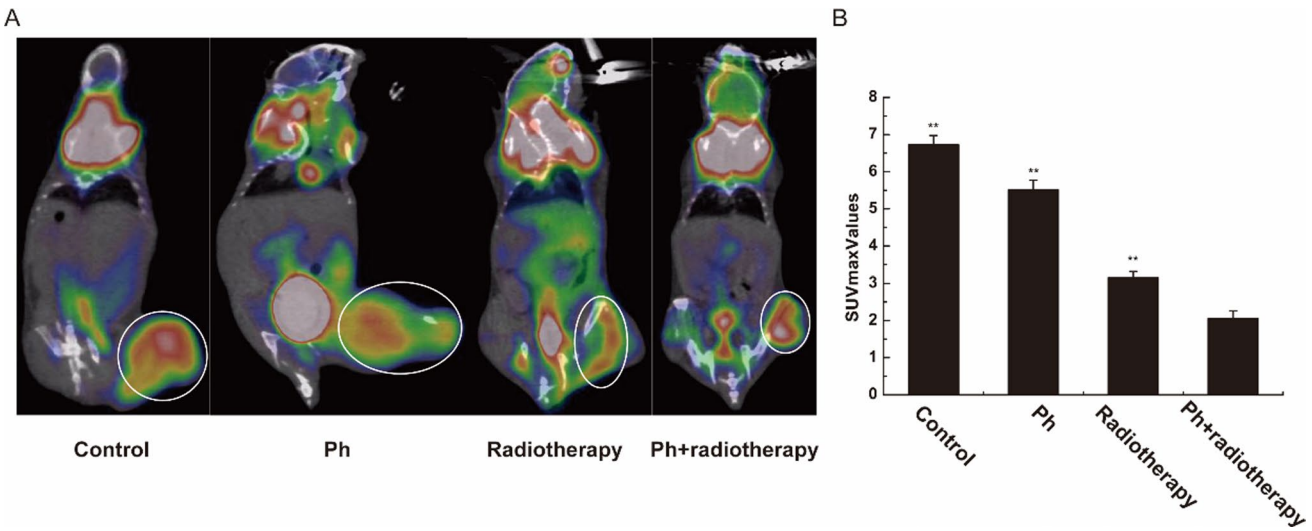

Fig. 4 ^{18}F-FDG PET/CT imaging. **A** Representative images of the mice after the last treatment. **B** The SUVmax values of ROI in four groups. $^{**}p < 0.01$

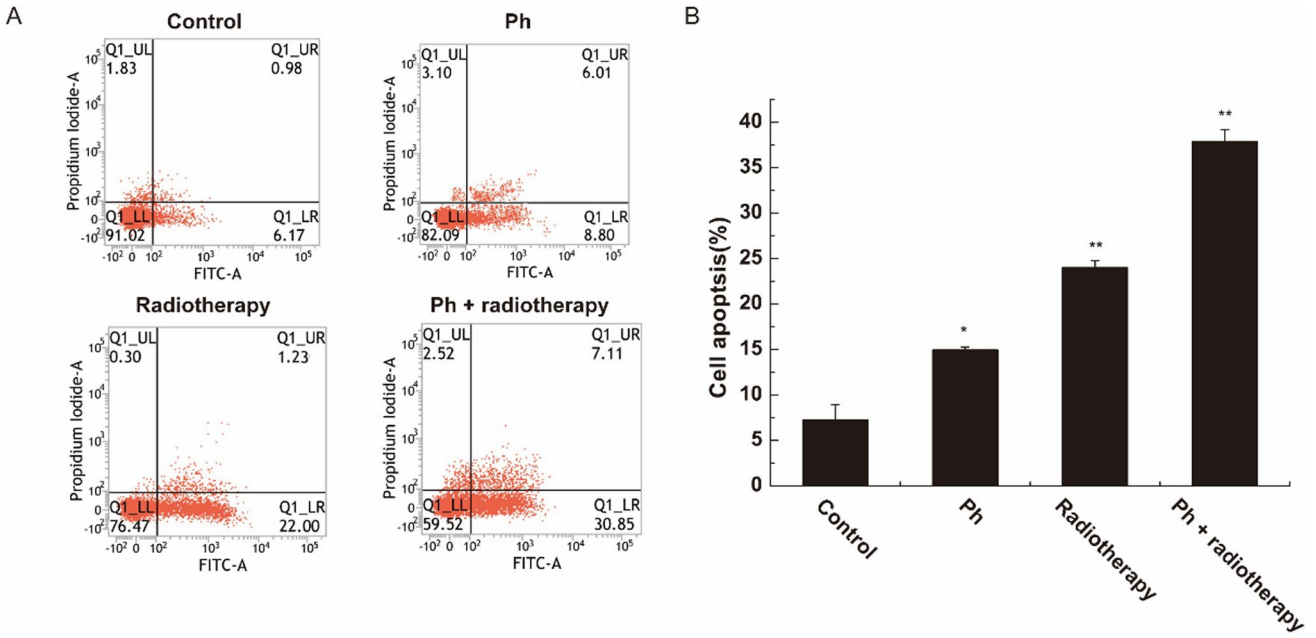

Fig. 5 The proportion of apoptotic cells in four groups. **A** Representative flow cytometry images of apoptotic cells in four groups. **B** Cell apoptosis rates in four groups. *$p < 0.05$, **$p < 0.01$

3.6 Ph combined with radiotherapy suppressed tumor cell proliferation

To evaluate the anti-proliferation effect, Ki-67 expression in the tumor cells was analyzed. The results showed that the percentage of Ki-67-positive cells in the combination of Ph and radiotherapy group was significantly decreased (Fig. 6A). Compared to the control group (45.29%), the percentage of Ki-67-positive cells were 23.10%, 14.72%, and 8.35% in the Ph alone, radiotherapy alone, and the combination of Ph and radiotherapy groups, respectively (Fig. 6B). These results indicated that Ph combined with radiotherapy significantly suppressed tumor cell proliferation.

4 Discussion

The management of lung cancer is complex, and radiotherapy serves as a therapeutic option in all stages of the disease and for patients in various clinical conditions [20]. However, the radiotoxicity results in treatment tolerability issues and affects the quality of life [21]. Therefore, combining anti-cancer drugs with radiotherapy to improve the efficacy of radiotherapy is an area of active study [22]. Ph, a dihydrochalcone, has exhibited anti-cancer properties in various cancers [8, 12, 13, 19]. This study aimed to investigate whether Ph could sensitize lung cancer to radiotherapy.

The results of this study demonstrated that Ph had anti-tumor effects, consistent with previous research findings [8]. We found that Ph inhibited the proliferation of LLC cells in a time- and dose-dependent manner. Furthermore, our results showed that the combination of Ph and radiotherapy inhibited colony formation of LLC cells. Concurrently, we discovered that the combination of Ph and radiotherapy, compared with Ph or radiotherapy alone, significantly inhibited tumor growth, prolonged the survival of mice, reduced tumor cell glucose transport, and increased tumor cell apoptosis. These findings suggested that Ph may enhance the sensitivity of tumor cells to radiotherapy.

High cellular glucose metabolism is recognized as one hallmark of cancer [23]. In an aerobic state, cancer cells increase glucose uptake for glycolysis and produce lactate to adapt to the microenvironment and maintain their proliferation, a phenomenon called the Warburg effect [24, 25]. Transmembrane transport mediated by GLUT proteins in tumor cells is the first rate-limiting step in glucose metabolism [26]. Targeting glucose metabolism and transportation has become a research focus for cancer therapeutic intervention [27–29]. Previous reports have identified Ph as a new type of small compound that suppresses the growth of cancer cells by inhibiting glucose transport and inducing glucose deprivation in hepatoma, colorectal, and triple-negative breast cancer [13, 30, 31]. In human liver cancer, a high level of GLUT2 was

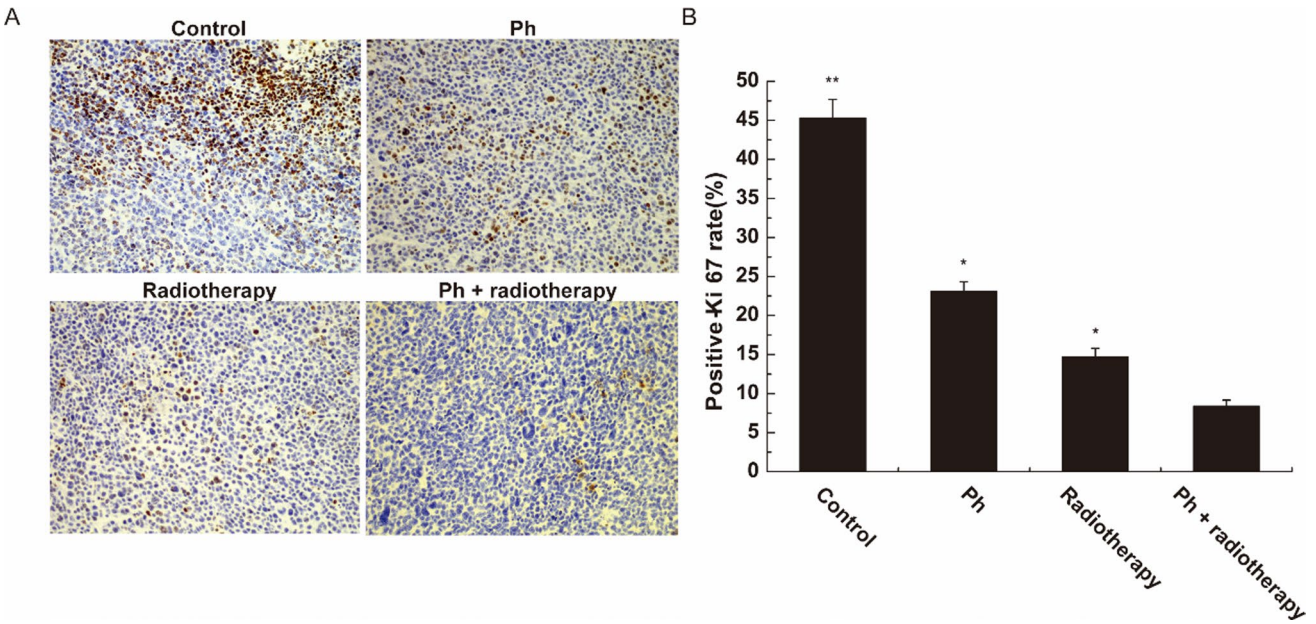

Fig. 6 Ki-67 expression in transplanted tumors from different groups. **A** Representative IHC images in four groups (400×). **B** The percentage of Ki-67 positive cells in four groups. *$p < 0.05$, **$p < 0.01$

observed in cell membranes [32]. In HepG2 tumor-bearing mice, ^{18}F-FDG uptake was significantly decreased in the Ph-treated group compared with controls, which may be due to the inhibition of GLUT2 glucose transport [32]. ^{18}F-FDG is used to measure glucose metabolism in vivo, and its accumulation reflects increased glucose consumption, which is usually associated with poor prognosis [33, 34]. In this study, Ph combined with radiotherapy significantly inhibited tumor growth and ^{18}F-FDG uptake. Our results suggested that Ph may have enhanced the killing effect of radiotherapy by inhibiting glucose transport. The inhibition of GLUT activity by Ph may also contribute to the enhanced radiosensitivity observed in this study. We speculate that when Ph inhibits GLUT proteins, such as GLUT2, the glucose uptake of cancer cells is reduced [35]. This could lead to a decrease in the energy supply of cancer cells, making them more vulnerable to the damaging effects of radiotherapy. Cancer cells require a large amount of energy to repair DNA damage caused by radiation [36]. With the inhibition of glucose transport or activity, the energy supply of cancer cells may become insufficient, which could impair their ability to repair radiation-induced damage and thus enhance their radiosensitivity.

Additionally, the inhibition of glucose transport can induce oxidative stress in cancer cells [37]. Under normal circumstances, cancer cells maintain a balance of reactive oxygen species (ROS) through glucose metabolism [38]. When glucose transport is inhibited, this balance is disrupted, leading to an increase in ROS levels [39]. The elevated ROS levels can further damage the DNA and other cellular components of cancer cells, thereby enhancing the therapeutic effect of radiotherapy [40].

Furthermore, decreased glucose transport and metabolism are associated with early apoptosis, including the mitochondrial death pathway induced by ATP depletion, oxidative stress-triggering cell death events, and hypoxia-inducible factor-1a (HIF-1a), which is related to p53-associated apoptosis [41]. Ph induced apoptosis in hepatoma cells through suppressing glucose transport and ATP production, leading to mitochondrial dysfunction and activation of downstream apoptotic pathways [32]. Ki-67 is a nuclear antigen associated with proliferation [42]. In this study, Ph combined with radiotherapy significantly reduced the percentage of Ki-67-positive cells in the tumor xenografts of mice, which was consistent with the MTT results. Moreover, the group treated with the combination of Ph and radiotherapy significantly enhanced cell apoptosis compared to either radiotherapy or Ph treatment alone. These findings indicated that Ph exerts radiosensitizing effects on lung cancer through the promotion of cell apoptosis and inhibition of tumor cell proliferation.

Our study has certain limitations. Firstly, only one lung cancer cell line, namely LLC, was used. Using additional cell lines could provide more comprehensive results. Secondly, we did not conduct in-depth mechanistic validation for GLUT inhibition by Ph. Future studies should include more cell lines and detailed exploration of the mechanisms involved.

5 Conclusion

In summary, our research results showed that the combination of Ph and radiotherapy significantly inhibited tumor growth and extended the survival time of tumor-bearing mice, demonstrating that Ph enhances the anti-tumor effect of radiotherapy on lung cancer. The potential mechanisms may be related to the inhibition of glucose transport, promotion of cell apoptosis, and inhibition of cell proliferation.

Acknowledgements None.

Author contributions Conceptualization, Project administration: Juan Tang, Weijie Xiong; Project administration: Hongyu Xu; Resources: Weijie Xiong, Xianguo Liu, Maolin Shi; Data curation: Juan Tang, Yuhui Shi; Data analysis, Formal analysis: Hongyu Xu, Yanxin Yu; Writing—Review & Editing: All authors.

Funding This study was supported by the Sichuan Hospital Association (S22034) and the General Medical Research Fund Project (TYYLKYJJ-2022-044).

Data availability The data in this study are available from the corresponding author upon reasonable request.

Declarations

Ethics approval and consent to participate All animal experiments were carried out following the guidelines of the Institutional Animal Care and Use Committee of West China Hospital, Sichuan University, and approved by Universal Medical 363 Hospital. All procedures were conducted in full compliance with the ARRIVE guidelines.

Consent for publication Not applicable.

Competing interests The authors declare no competing interests.

References

1. Pelosi G, Pasini F. Over-time risk of lung cancer is largely owing to continuing smoking exposition: a good reason to quit. J Thorac Oncol. 2021;16:e57–9. https://doi.org/10.1016/j.jtho.2021.04.013.
2. Sung H, Ferlay J, Siegel RL, Laversanne M, Soerjomataram I, Jemal A, et al. Global Cancer Statistics 2020: GLOBOCAN estimates of incidence and mortality worldwide for 36 cancers in 185 countries. CA Cancer J Clin. 2021;71:209–49. https://doi.org/10.3322/caac.21660.
3. Bray F, Laversanne M, Sung H, Ferlay J, Siegel RL, Soerjomataram I, et al. Global cancer statistics 2022: GLOBOCAN estimates of incidence and mortality worldwide for 36 cancers in 185 countries. CA Cancer J Clin. 2024;74:229–63. https://doi.org/10.3322/caac.21834.
4. Thai AA, Solomon BJ, Sequist LV, Gainor JF, Heist RS. Lung cancer. Lancet. 2021;398:535–54. https://doi.org/10.1016/s0140-6736(21)00312-3.
5. Hirsch FR, Scagliotti GV, Mulshine JL, Kwon R, Curran WJ Jr, Wu YL, et al. Lung cancer: current therapies and new targeted treatments. Lancet. 2017;389:299–311. https://doi.org/10.1016/s0140-6736(16)30958-8.
6. Zhuang M, Jiang S, Gu A, Chen X, Mingyan E. Radiosensitizing effect of gold nanoparticle loaded with small interfering RNA-SP1 on lung cancer: AuNPs-si-SP1 regulates GZMB for radiosensitivity. Transl Oncol. 2021;14:101210. https://doi.org/10.1016/j.tranon.2021.101210.
7. Mariadoss AVA, Vinyagam R, Rajamanickam V, Sankaran V, Venkatesan S, David E. Pharmacological aspects and potential use of phloretin: a systemic review. Mini Rev Med Chem. 2019;19:1060–7. https://doi.org/10.2174/1389557519666190311154425.
8. Tuli HS, Rath P, Chauhan A, Ramniwas S, Vashishth K, Varol M, et al. Phloretin, as a potent anticancer compound: from chemistry to cellular interactions. Molecules. 2022;27:8819. https://doi.org/10.3390/molecules27248819.
9. Nakhate KT, Badwaik H, Choudhary R, Sakure K, Agrawal YO, Sharma C, et al. Therapeutic potential and pharmaceutical development of a multitargeted flavonoid phloretin. Nutrients. 2022;14:3638. https://doi.org/10.3390/nu14173638.

10. Kapoor S, Padwad YS. Phloretin induces G2/M arrest and apoptosis by suppressing the β-catenin signaling pathway in colorectal carcinoma cells. Apoptosis. 2023;28:810–29. https://doi.org/10.1007/s10495-023-01826-4.
11. Zhou M, Zheng J, Bi J, Wu X, Lyu J, Gao K. Synergistic inhibition of colon cancer cell growth by a combination of atorvastatin and phloretin. Oncol Lett. 2018;15:1985–92. https://doi.org/10.3892/ol.2017.7480.
12. Kim JL, Lee DH, Pan CH, Park SJ, Oh SC, Lee SY. Role of phloretin as a sensitizer to TRAIL-induced apoptosis in colon cancer. Oncol Lett. 2022;24:321. https://doi.org/10.3892/ol.2022.13441.
13. Wu KH, Ho CT, Chen ZF, Chen LC, Whang-Peng J, Lin TN, et al. The apple polyphenol phloretin inhibits breast cancer cell migration and proliferation via inhibition of signals by type 2 glucose transporter. J Food Drug Anal. 2018;26:221–31. https://doi.org/10.1016/j.jfda.2017.03.009.
14. Kang J, Kim E, Kim W, Seong KM, Youn H, Kim JW, et al. Rhamnetin and cirsiliol induce radiosensitization and inhibition of epithelial-mesenchymal transition (EMT) by miR-34a-mediated suppression of Notch-1 expression in non-small cell lung cancer cell lines. J Biol Chem. 2013;288:27343–57. https://doi.org/10.1074/jbc.M113.490482.
15. Arefnezhad R, Amin SS, Mohammdi A, Ahmadi G, Jahandideh A, Goleij P, et al. Quercetin and its nanoformulations as promising agents for lung cancer treatment: a focus on molecular mechanisms. J Drug Deliv Sci Technol. 2024;99: 105933. https://doi.org/10.1016/j.jddst.2024.105933.
16. Du Y, Jia C, Liu Y, Li Y, Wang J, Sun K. Isorhamnetin enhances the radiosensitivity of A549 cells through interleukin-13 and the NF-ÎşB signaling pathway. Front Pharmacol. 2020;11: 610772. https://doi.org/10.3389/fphar.2020.610772.
17. Tang J, Wang N, Wu J, Ren P, Li J, Yang L, et al. Synergistic effect and reduced toxicity by intratumoral injection of cytarabine-loaded hyaluronic acid hydrogel conjugates combined with radiotherapy on lung cancer. Invest New Drugs. 2019;37:1146–57. https://doi.org/10.1007/s10637-019-00740-4.
18. Hsiao YH, Hsieh MJ, Yang SF, Chen SP, Tsai WC, Chen PN. Phloretin suppresses metastasis by targeting protease and inhibits cancer stemness and angiogenesis in human cervical cancer cells. Phytomedicine. 2019;62: 152964. https://doi.org/10.1016/j.phymed.2019.152964.
19. Min J, Huang K, Tang H, Ding X, Qi C, Qin X, et al. Phloretin induces apoptosis of non-small cell lung carcinoma A549 cells via JNK1/2 and p38 MAPK pathways. Oncol Rep. 2015;34:2871–9. https://doi.org/10.3892/or.2015.4325.
20. Vinod SK, Hau E. Radiotherapy treatment for lung cancer: current status and future directions. Respirology. 2020;25(Suppl 2):61–71. https://doi.org/10.1111/resp.13870.
21. De Ruysscher D, Niedermann G, Burnet NG, Siva S, Lee AWM, Hegi-Johnson F. Radiotherapy toxicity. Nat Rev Dis Primers. 2019;5:13. https://doi.org/10.1038/s41572-019-0064-5.
22. Citrin DE. Recent developments in radiotherapy. N Engl J Med. 2017;377:1065–75. https://doi.org/10.1056/NEJMra1608986.
23. Hay N. Reprogramming glucose metabolism in cancer: can it be exploited for cancer therapy? Nat Rev Cancer. 2016;16:635–49. https://doi.org/10.1038/nrc.2016.77.
24. Li S, Zeng H, Fan J, Wang F, Xu C, Li Y, et al. Glutamine metabolism in breast cancer and possible therapeutic targets. Biochem Pharmacol. 2023;210: 115464. https://doi.org/10.1016/j.bcp.2023.115464.
25. Abdel-Wahab AF, Mahmoud W, Al-Harizy RM. Targeting glucose metabolism to suppress cancer progression: prospective of anti-glycolytic cancer therapy. Pharmacol Res. 2019;150:104511. https://doi.org/10.1016/j.phrs.2019.104511.
26. Barron CC, Bilan PJ, Tsakiridis T, Tsiani E. Facilitative glucose transporters: implications for cancer detection, prognosis and treatment. Metabolism. 2016;65:124–39. https://doi.org/10.1016/j.metabol.2015.10.007.
27. Zhang H-L, Wang M-D, Zhou X, Qin C-J, Fu G-B, Tang L, et al. Blocking preferential glucose uptake sensitizes liver tumor-initiating cells to glucose restriction and sorafenib treatment. Cancer Lett. 2017;388:1–11. https://doi.org/10.1016/j.canlet.2016.11.023.
28. Abdel-Wahab AF, Mahmoud W, Al-Harizy RM. Targeting glucose metabolism to suppress cancer progression: prospective of anti-glycolytic cancer therapy. Pharmacol Res. 2019;150: 104511. https://doi.org/10.1016/j.phrs.2019.104511.
29. Narayanan K, Erathodiyil N, Gopalan B, Chong S, Wan ACA, Ying JY. Targeting warburg effect in cancers with PEGylated glucose. Adv Healthc Mater. 2016;5:696–701. https://doi.org/10.1002/adhm.201500613.
30. Lin ST, Tu SH, Yang PS, Hsu SP, Lee WH, Ho CT, et al. Apple polyphenol phloretin inhibits colorectal cancer cell growth via inhibition of the type 2 glucose transporter and activation of p53-mediated signaling. J Agric Food Chem. 2016;64:6826–37. https://doi.org/10.1021/acs.jafc.6b02861.
31. Elmetwalli A, Kamosh NH, El Safty R, Youssef AI, Salama MM, Abd El-Razek KM, et al. Novel phloretin-based combinations targeting glucose metabolism in hepatocellular carcinoma through GLUT2/PEPCK axis of action: in silico molecular modelling and in vivo studies. Med Oncol. 2023;41:12. https://doi.org/10.1007/s12032-023-02236-x.
32. Wu CH, Ho YS, Tsai CY, Wang YJ, Tseng H, Wei PL, et al. In vitro and in vivo study of phloretin-induced apoptosis in human liver cancer cells involving inhibition of type II glucose transporter. Int J Cancer. 2009;124:2210–9. https://doi.org/10.1002/ijc.24189.
33. Salas JR, Clark PM. Signaling pathways that drive (18)F-FDG accumulation in cancer. J Nucl Med. 2022;63:659–63. https://doi.org/10.2967/jnumed.121.262609.
34. Sugita S, Yamato M, Hatabu T, Kataoka Y. Involvement of cancer-derived EMT cells in the accumulation of (18)F-fluorodeoxyglucose in the hypoxic cancer microenvironment. Sci Rep. 2021;11:9668. https://doi.org/10.1038/s41598-021-88414-1.
35. Zhan T, Digel M, Kăźch EM, Stremmel W, Făźllekrug J. Silybin and dehydrosilybin decrease glucose uptake by inhibiting GLUT proteins. J Cell Biochem. 2011;112:849–59. https://doi.org/10.1002/jcb.22984.
36. Sun F, Li W, Du R, Liu M, Cheng Y, Ma J, et al. Impact of glycolysis enzymes and metabolites in regulating DNA damage repair in tumorigenesis and therapy. Cell Commun Signal. 2025;23:44. https://doi.org/10.1186/s12964-025-02047-9.
37. Komza M, Khatun J, Gelles JD, Trotta AP, Abraham-Enachescu I, Henao J, et al. Metabolic adaptations to acute glucose uptake inhibition converge upon mitochondrial respiration for leukemia cell survival. Cell Commun Signal. 2025;23:47. https://doi.org/10.1186/s12964-025-02044-y.
38. Hayes JD, Dinkova-Kostova AT, Tew KD. Oxidative Stress in Cancer. Cancer Cell. 2020;38:167–97. https://doi.org/10.1016/j.ccell.2020.06.001.

39. Shriwas P, Roberts D, Li Y, Wang L, Qian Y, Bergmeier S, et al. A small-molecule pan-class I glucose transporter inhibitor reduces cancer cell proliferation in vitro and tumor growth in vivo by targeting glucose-based metabolism. Cancer Metab. 2021;9:14. https://doi.org/10.1186/s40170-021-00248-7.
40. An X, Yu W, Liu J, Tang D, Yang L, Chen X. Oxidative cell death in cancer: mechanisms and therapeutic opportunities. Cell Death Dis. 2024;15:556. https://doi.org/10.1038/s41419-024-06939-5.
41. Zeng C, Zhang Z, Luo W, Wang L, Zhou H, Nie C. JNK initiates Beclin-1 dependent autophagic cell death against Akt activation. Exp Cell Res. 2022;414: 113105. https://doi.org/10.1016/j.yexcr.2022.113105.
42. Menon SS, Guruvayoorappan C, Sakthivel KM, Rasmi RR. Ki-67 protein as a tumour proliferation marker. Clin Chim Acta. 2019;491:39–45. https://doi.org/10.1016/j.cca.2019.01.011.